Am J Cancer Res 2023;13(6):2410-2425
www.ajcr.us /ISSN:2156-6976/ajcr0150714

Original Article

THOC2 expression and its impact on 5-fluorouracil resistance in glioblastoma multiforme

Young Jun Lee[1,2], Jin-Hwa Jung[1,3], Da-Young Chang[1,3], Min Gyeong Kim[1,2], Narayan Bashyal[1,3], Woo Sup Hwang[1], Hyun Goo Woo[4], Sun Ha Paek[5], Haeyoung Suh-Kim[1,3], Sung-Soo Kim[1]

[1]Department of Anatomy, Ajou University School of Medicine, Suwon, South Korea; [2]Department of Biomedical Sciences, Ajou University Graduate School of Medicine, Suwon, South Korea; [3]Research Center, Cell&Brain, Suwon, South Korea; [4]Department of Physiology, Ajou University School of Medicine, Suwon, South Korea; [5]Department of Neurosurgery, Seoul National University College of Medicine, Seoul, South Korea

Received April 13, 2023; Accepted May 20, 2023; Epub June 15, 2023; Published June 30, 2023

Abstract: Glioblastoma multiforme (GBM) is a highly aggressive brain tumor with poor prognosis and limited treatment options. While 5-fluorouracil (5-FU) has not been widely employed in GBM therapy, emerging research indicates its potential for effectiveness when combined with advanced drug delivery systems to improve its transport to brain tumors. This study aims to investigate the role of THOC2 expression in 5-FU resistance in GBM cell lines. We evaluated diverse GBM cell lines and primary glioma cells for 5-FU sensitivity, cell doubling times, and gene expression. We observed a significant correlation between THOC2 expression and 5-FU resistance. To further investigate this correlation, we selected five GBM cell lines and developed 5-FU resistant GBM cells, including T98FR cells, through long-term 5-FU treatment. In 5-FU challenged cells, THOC2 expression was upregulated, with the highest increase in T98FR cells. THOC2 knockdown in T98FR cells reduced 5-FU IC50 values, confirming its role in 5-FU resistance. In a mouse xenograft model, THOC2 knockdown attenuated tumor growth and extended survival duration after 5-FU treatment. RNA sequencing identified differentially expressed genes and alternative splicing variants in T98FR/shTHOC2 cells. THOC2 knockdown altered Bcl-x splicing, increasing pro-apoptotic Bcl-xS expression, and impaired cell adhesion and migration by reducing L1CAM expression. These results suggest that THOC2 plays a crucial role in 5-FU resistance in GBM and that targeting THOC2 expression could be a potential therapeutic strategy for improving the efficacy of 5-FU-based combination therapies in GBM patients.

Keywords: THOC2, glioblastoma, chemotherapy resistance, 5-fluorouracil (5-FU), tumor formation, therapeutic target

Introduction

Glioblastoma multiforme (GBM) is a highly aggressive and prevalent type of brain tumor that affects adults, characterized by rapid growth, diffuse infiltration, and poor prognosis [1]. With an incidence rate of 3.2 cases per 100,000 individuals, GBM accounts for around 50% of all primary malignant brain tumors [2]. Patients with GBM often experience symptoms such as headaches, seizures, and cognitive impairments due to increased intracranial pressure and the spread of the tumor into healthy brain tissue. Despite advances in surgical techniques, radiotherapy, chemotherapy, targeted therapies, immunotherapies, and tumor-treating fields (TTFields), the median survival for GBM patients remains around 14-16 months [3-5].

The current treatments for GBM face challenges, such as the location of the tumor, the blood-brain barrier, and the development of resistance [6-8]. 5-fluorouracil (5-FU) is a widely used anticancer drug, primarily for gastrointestinal malignancies, that works by inhibiting thymidylate synthase and disrupting RNA and DNA synthesis and function [9, 10]. 5-FU has demonstrated potential in treating various types of cancer, but it is not commonly used as a standard treatment for GBM. Understanding the factors influencing its reactivity and resistance

could provide valuable insights for optimizing alternative strategies and improving patient outcomes.

Recent studies have demonstrated the potential of 5-FU as an effective therapeutic agent when delivered to brain tumors through advanced drug delivery systems, such as nanoparticles [9, 10] or liposomes [11]. In addition, gene therapy for GBM has been attempted [12], and an *ex vivo* treatment is also under development [13]. In a previous study, we developed a brain tumor-specific therapy using cytosine deaminase expressing mesenchymal stem cells and 5-fluorocytosine [13, 14]. This therapy, combined with other therapies like radiotherapy or temozolomide, could decrease GBM recurrence by removing residual cancer cells after surgical resection. However, this therapy also has limitations, as its efficacy could be decreased if tumor cells are resistant to 5-FU or acquire resistance during treatment.

By investigating the genes responsible for 5-FU resistance in GBM, we could predict the efficacy of our therapy or even find ways to neutralize its resistance. This deeper understanding of the factors influencing the reactivity and resistance of 5-FU in the context of GBM could contribute to the development of more effective alternative strategies, ultimately leading to improved patient outcomes.

The relationship between THOC2, a component of the TREX complex involved in mRNA export from the nucleus to the cytoplasm [15, 16], and 5-FU resistance in GBM remains unclear. The TREX complex plays a critical role in various cellular processes, including transcription, splicing, and mRNA stability, which have been linked to tumorigenesis and chemoresistance in various types of cancer [17, 18]. However, the molecular mechanisms through which THOC2 may influence 5-FU resistance, including alternative splicing events and the regulation of cell-adhesion-related genes, have yet to be determined.

In this study, we aim to examine the association between THOC2 expression and 5-FU reactivity in GBM cell lines and to investigate the functional consequences of THOC2 suppression on 5-FU resistance, tumor formation, and cell-adhesion using both experimental models. Our investigation will include an analysis of the expression of known resistance-related genes, such as dihydropyrimidine dehydrogenase (DPYD) and thymidylate synthase (TS) [19], as well as THOC2, in relation to 5-FU reactivity. Additionally, we will explore the potential molecular mechanisms through which THOC2 may influence 5-FU resistance, including alternative splicing events and the regulation of cell-adhesion-related genes.

By investigating THOC2 in the context of GBM and 5-FU resistance, our study aims to deepen our understanding of the molecular mechanisms underlying chemoresistance in GBM and to inform the development of more effective therapeutic strategies for GBM patients. This could include gene therapy and gene cell therapy approaches targeting similar pathways to enhance their efficacy in treating GBM [13, 14, 20]. Our research will contribute to the existing knowledge on GBM chemoresistance and guide future research efforts in this area, by providing a comprehensive analysis of the relationship between THOC2 expression and 5-FU reactivity and the potential molecular mechanisms involved in this association.

Materials and methods

Cell culture

Human glioblastoma cell lines A172, U87MG, T98G, U373MG, SNU201, SNU489, SNU626, and SNU738 were obtained from the Korea Cell Line Bank (Seoul, Korea), while LN229 was acquired from the American Type Culture Collection (ATCC, Rockville, MD). Additionally, primary glioblastoma cell lines GBL28, GBL37, GBL67, and GBL68 were generated at Seoul National University Hospital (IRB No. 1009-025-331). All cells were cultured in a humidified 37°C incubator with 5% CO_2. The culture media consisted of Dulbecco's Modified Eagle Medium (DMEM) supplemented with 10% FBS, 100 U/mL penicillin, and 100 μg/mL streptomycin (Invitrogen, Carlsbad, CA, USA). 5-FU resistant GBM cells were developed by exposing parental GBM cells to a 5 μM dose of 5-FU (Sigma-Aldrich, St. Louis, MO, USA) for four cell lines and 1 μM for the A172 cell line for 12 months.

5-FU toxicity test by MTT assay

Cells were plated in a 96-well plate at a density of 2,000 cells/well. After culturing in standard

Table 1. Primer list for RT-qPCR

Gene	Sequence (5' to 3')	Product length (bp)
TS	F: TTGGAGGAGTTGCTGTGG	337
	R: CGTAGCTGGCGATGTTGA	
DPYD	F: CAGAAGAGCTGTCCAACTAA	310
	R: CAAATAGGAGACGTCAGAGAG	
THOC2	F: GGAGCAACTAGAGGCTATGACTG	155
	R: GCTGAGCCATAAGCAGACAGAG	
GAPDH	F: GTCTCCTCTGACTTCAACAGCG	131
	R: ACCACCCTGTTGCTGTAGCCAA	
Bcl-x [50]	F: AGTAAAGCAAGCGCTGAGGGAG	452 (Bcl-xL), 250 (Bcl-xS)
	R: ACTGAAGAGTGAGCCCAGCAGA	
*Bcl-x*S [51]	F: GCAGTAAAGCAAGCGCTGAG	267
	R: GTTCCACAAAAGTATCCTGTTCAAAG	

growth medium for 24 hours, the old medium was replaced with fresh growth medium containing indicated concentrations of 5-FU every 48 hours. On the fifth day, survival rates of the cells were measured with 3-[4,5-dimethylthiazol-2-yl]-2,5-diphenyltetrazolium bromide (MTT) assay (Sigma-Aldrich). Briefly, cells were incubated in 200 μL of MTT for 2 hours. Formazan crystals were then solubilized with 100 μL of DMSO, and the absorbance at OD 540 was measured using an ID3 spectrophotometer (Molecular Devices, San Jose, CA, USA). The absorbance at each concentration was expressed relative to that of the untreated control cells as the mean ± SEM of three independent experiments. The half-maximal inhibitory concentration (IC50) values were calculated by fitting the curve using the Sigmaplot 12.5 program (Systat Software Inc., San Jose, CA, USA).

Growth kinetics

Cells were plated on a 6-well plate at a density of 50,000 cells per well and were maintained in Dulbecco's modified Eagle medium supplemented with 10% FBS, 100 U/mL penicillin, and 100 μg/mL streptomycin in a 37°C incubator. From the first day to the fifth day, the cells were washed with PBS and detached using Trypsin-EDTA. The detached cells were then resuspended in standard growth medium, and the cell numbers were counted using trypan blue and Countess™ II automated cell counter (Life technologies, Carlsbad, CA, USA).

RT-qPCR

Total RNA was isolated from cells using a Hybrid-RTM 100p RNA isolation kit (GeneAll, Seoul, Korea), and cDNA was synthesized using the SuperScript™ IV First-Strand Synthesis System (Invitrogen). Amplification was performed using a Power SYBRTM green PCR master mix (Applied Biosystems, part of Thermo Fisher Scientific, Waltham, MA, USA) and 1/20 of the volume of the first-strand cDNA reaction mixture using the Step One PlusTM (Applied Biosystems). The primers used in RT-qPCR are listed in **Table 1**.

Lentivirus transduction

The green fluorescence protein (GFP) expressing THOC2 shRNA lentiviral vector TL301111 (Origene, Rockville, MD, USA) and control scrambled vector (TR30021, Origene) were transduced to T98FR with 8 μg/mL polybrene (Sigma-Aldrich).

THOC2 western blot

Cells were lysed using a standard protocol in RIPA buffer (Thermo-Fisher, Waltham, USA) and separated on precast (Mini-PROTEAN TGX precast gels, Bio-Rad, Hercules, CA, USA) for western analysis of THOC2 and actin. After transfer to a polyvinylidene difluoride membrane (Bio-Rad), the proteins were probed with anti-THOC2 (1:1,000, Thermo-Fisher) or anti-actin (1:1,000, Millipore, Burlington, USA) antibodies and visualized using HRP (horseradish peroxidase)-conjugated anti-rabbit or anti-mouse IgG antibodies (1:50,000, Thermo-Fisher) and SuperSignal West Atto Substrate (Thermo-Fisher).

In vivo anticancer activity

Animal protocols were approved by the Institutional Animal Care and Use Committee of Ajou University Medical School. Eight-week-old male NOD.Cg-Prkdcscid Il2rgtm1Wjl/SzJ (Jackson Laboratory, Bar Harbor, ME, USA)

were anesthetized and inoculated with T98FR/sc or T98FR/shTHOC2 cells (1.5 × 10^6 cells/100 μL) in the right flank, along with a 20% volume of Matrigel (Corning, New York, USA). Once the tumor reached a volume of 100-200 mm^3, mice were administered with 80 mg/kg of 5-FU via peritumoral subcutaneous injection once a week for three consecutive weeks. Tumor volume was measured every week using a Vernier caliper. The formula used for measuring tumor volume (mm^3) was (π/6) * (length * width * height).

RNA sequencing and analysis

Total RNA was isolated using the Hybrid-RTM 100p RNA isolation kit (GeneAll) and sent to Macrogen (Seoul, Korea) for quality control and RNA sequencing. Library preparation was performed using the Illumina TruSeq standard mRNA LT sample prep kit, following the manufacturer's instructions. Sequencing was carried out using NovaSeq6000 (Illumina, San Diego, CA, USA). After preprocessing, the trimmed reads were mapped to the GRCh37 reference genome using HISAT2, and transcript assembly was performed using StringTie. The expression profiles of known transcripts per sample were acquired and converted to read count, FPKM (fragment per kilobase of transcript per million mapped reads), and TPM (transcripts per kilobase million) based on transcript/gene.

To investigate transcriptome changes between T98FR/sc and T98FR/shTHOC2, we identified differentially expressed genes (DEGs) exhibiting a fold change of 2 or greater and a *p*-value of 0.05 or lower using edgeR [21]. Subsequently, gene set enrichment analysis was performed on the extracted DEG list employing gProfiler [22]. The top 10 significantly decreased genes were extracted by sorting the *p* values of quasi-likelihood F test for cell adhesion genes identified from edgeR in ascending order. The top 10 significantly downregulated genes were obtained by sorting the *p*-values of the quasi-likelihood F test for cell adhesion genes, as identified by edgeR, in ascending order. For alternative splicing variant analysis, we calculated the correlation coefficients between each sample's 5-FU IC50 value and the average FPKM of transcripts using the PEARSON function in Microsoft Excel (Microsoft, Redmond, WA, USA). The gene list containing significantly correlated genes was further analyzed using DAVID functional annotation [23, 24]. Lastly, a hierarchical clustering heatmap of T98FR/sc, T98FR/shTHOC2, and T98G was generated using the iDEP web application version .96 [25].

Immunohistochemistry

Animals were perfused with 4% paraformaldehyde (PFA) one week after the final 5-FU administration. Subcutaneous tumors were extracted and fixed with 4% PFA at 4°C for one week. Next, tumors were processed with paraffin using a TP 1020 tissue processor (Leica, Wetzlar, Germany). Paraffin-fixed tumors were sectioned at a 5 μm thickness and placed on slides. Slides were incubated at 60°C for 2 hours, deparaffinized, rehydrated, and stored in distilled water for 20 minutes. For immunohistochemical staining, antigen retrieval was performed on rehydrated slides with boiling 0.01 M sodium citrate (pH 6.0, Sigma) for 30 minutes. Once cooled, slides were permeabilized with 0.1% Triton-X 100 (Sigma) in PBS for 60 minutes and blocked with 10% normal horse serum for 1 hour. Slides were incubated with anti-L1CAM antibody (1:200, ab24345, Abcam, Cambridge, UK) for 2 hours at room temperature. Slides were then washed with PBS-T for 10 minutes and treated with biotinylated secondary antibody (1:200, BA-2000, Vector Laboratories, Burlingame, USA) for 1 hour. After washing with PBS for 10 minutes, slides were treated with Vectastain ABC kits (Vector Laboratories) for 30 minutes. ABC-treated slides were washed with PBS for 10 minutes and treated with 0.5 mg/mL 3,3'-diaminobenzidine (DAB) (Sigma-Aldrich) substrate for oxidation. The slides were then counter-stained with Gill's hematoxylin II (BBC biochemical, McKinney, TX, USA). Slides were mounted using Fluoromount-G™ Mounting Medium (SouthernBiotech, Birmingham, CA, USA) and imaged with an IX71 inverted microscope (Olympus, Tokyo, Japan).

Cell attachment assay

A 96-well plate was coated with Matrigel by adding DMEM with 10% Matrigel 354230 (Corning) to a 24-well plate and incubating it for 2 hours in a 37°C incubator. Cells were plated on Matrigel-coated wells at a concentration of

10,000 cells per well. Four hours later, the non-attached cells were removed by washing the plates three times with PBS. The attached cells were fixed with methanol for 20 min and stained with 0.1% crystal violet (Sigma-Aldrich) solution. Stained cells in three randomly selected fields were imaged using an IX71 inverted microscope (Olympus) and analyzed using ImageJ 1.53t (National Institute of Health, Rockville, MD, USA).

Wound healing assay

T98FR/sc and T98FR/shTHOC2 cells were seeded into a 24-well culture plate and cultivated for 24 hours to achieve complete spreading of cells and 100% confluency. The cells were then serum-starved for 24 hours in DMEM containing 0.1% FBS and 1% P/S. After serum starvation, wounds were generated by scratching the confluent cell sheet with a 200 µL pipette tip. The wounded cell culture was washed with PBS and then incubated for 24 hours with DMEM containing 0.1% FBS and 1% P/S. Pictures of the cell culture were taken using an IX71 inverted microscope camera (Olympus), and the recovered wounded area was analyzed using ImageJ 1.53t (National Institute of Health) and the wound healing size tool plugin.

Statistical analysis

All *in vitro* results are based on at least three independent experiment replicates. The student's t-test was used to calculate the statistical significance in the comparison of *in vitro* results and *in vivo* tumor volume. The log-rank test was used to determine the statistical significance between the survival of animals in the *in vivo* assay. The results are expressed as the mean ± standard deviation (SD).

Results

Variation in 5-FU reactivity, growth rate, and gene expression in GBM cell lines

We acquired diverse glioblastoma cell lines and primary glioma cells and examined their sensitivity to 5-FU, cell doubling times, and gene expression during cell culture and 5-FU toxicity tests (**Figure 1A**, **1B**). The sensitivity to 5-FU was determined by generating dose-response curves across a range of concentrations in triplicate experiments, from which the IC50 values were calculated (detailed dose-response curves are provided in Supplementary Figure 1). We conducted a linear regression analysis to determine the correlation between cell doubling times and 5-FU IC50 values for GBM and primary glioma cells (**Figure 1C**). Using RT-qPCR, we determined the relative mRNA expression levels of THOC2, TS (thymidylate synthase), and DPYD (dihydropyrimidine dehydrogenase) and correlated them with 5-FU IC50 values (**Figure 1D-F**). We calculated the coefficient of determination (R^2) for each regression line using Pearson's formula, with THOC2 displaying the highest R^2 value of 0.6414. Statistical analysis was performed using Pearson's correlation coefficient, and a p-value < 0.05 was considered statistically significant.

THOC2 expression correlates with 5-FU resistance in GBM cell lines

To further investigate the correlation between 5-FU resistance and THOC2 expression, we selected five GBM cell lines (A172, U87MG, T98G, U373MG, SNU738) with varying baseline 5-FU sensitivities, molecular characteristics, and genetic backgrounds. We cultured these cell lines with a concentration of 5 µM 5-FU for four of the GBM cell lines and 1 µM 5-FU for the highly sensitive A172 cell line for 12 months to simulate 5-FU treatment during chemotherapy and develop 5-FU resistant GBM (FR) cells. The 5-FU challenged GBM cells exhibited increased 5-FU IC50 values compared to the original cells. The 5-FU treated T98G cells had the most increased 5-FU IC50 value, from 12.2 µM to 61.2 µM (**Figure 2A**). We used RT-qPCR to determine the relative mRNA expression levels between 5-FU challenged and original cells. 5-FU challenge increased the expression of THOC2 in all cells except A172. In particular, T98FR (5-FU challenged T98G), where the IC50 increased the most, also showed the highest increase of 1.6-fold (**Figure 2B**). We also performed a Pearson correlation analysis between 5-FU IC50 and THOC2 mRNA expression before and after of 5-FU challenge (**Figure 2C**). The result indicates a strong positive correlation in both original cells (correlation coefficient = 0.6890, p-value = 0.0001) and 5-FU challenged cells (correlation coefficient = 0.8302, p-value < 0.0001).

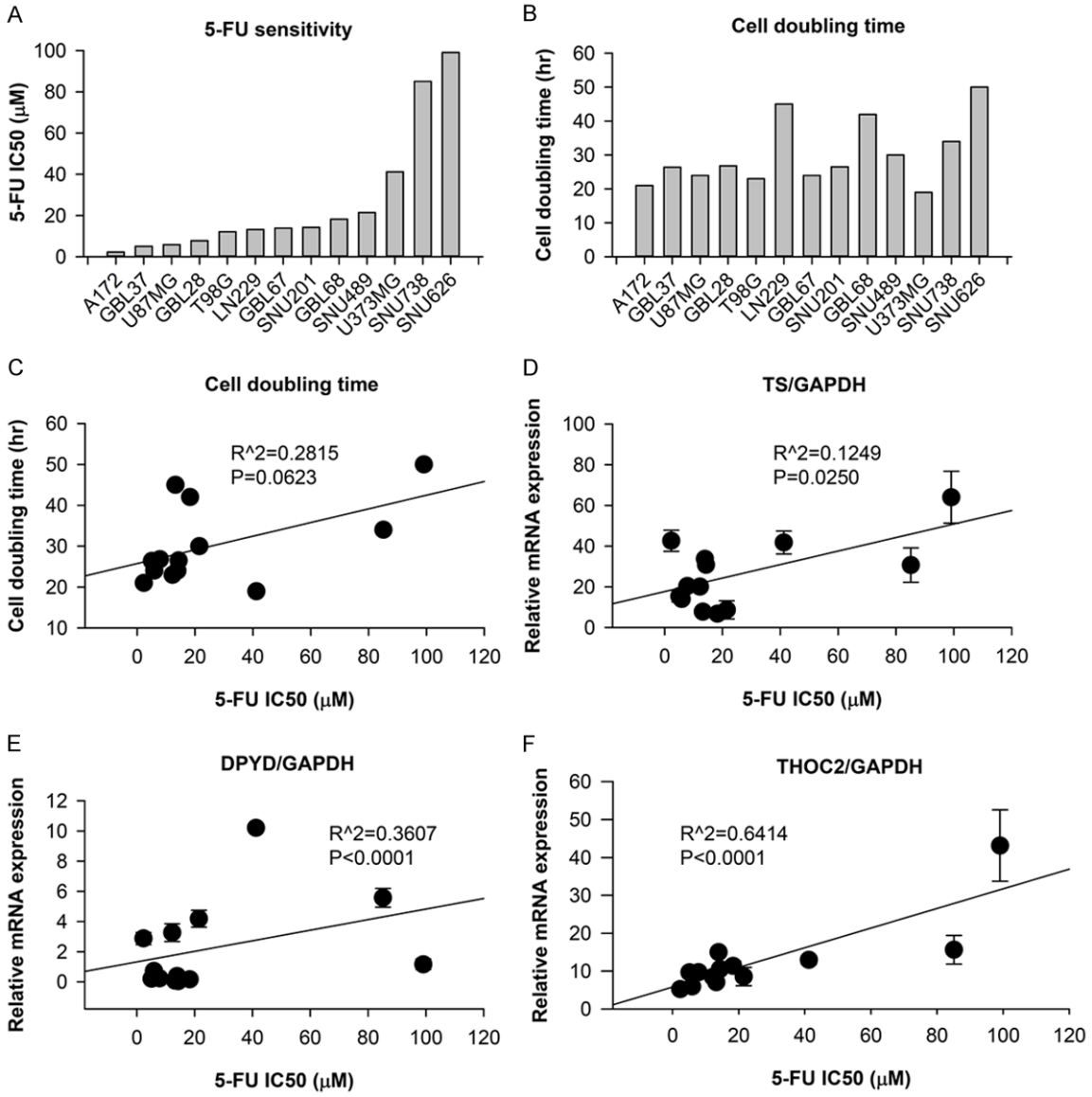

Figure 1. Correlation between 5-FU sensitivity, cell doubling time, and mRNA expression levels of 5-FU metabolism genes. A, B. Various GBM cells were obtained, and their 5-FU IC50 values and cell doubling times were determined. C. Linear regression was performed to correlate cell doubling time with 5-FU IC50 values, and R^2 values were calculated using Pearson's correlation coefficient formula. D-F. Relative mRNA expression levels of 5-FU metabolism genes and THOC2 were measured by quantitative RT-qPCR. Linear regression was performed to correlate mRNA expression levels of 5-FU metabolism genes with 5-FU IC50 values.

This finding substantiates our statement about the correlation between 5-FU resistance and THOC2 expression.

To confirm THOC2's effect on 5-FU resistance in T98FR, we transiently transduced T98FR cells with shTHOC2 expressing lentiviruses. Although there were no significant differences in growth rate after THOC2 knockdown, the 5-FU toxicity test results showed that THOC2 knockdown decreased the 5-FU sensitivity of T98FR, reducing the 5-FU IC50 from 61.2 μM to 39.3 μM (**Figure 2D**, **2E**). We confirmed inhibited THOC2 mRNA and protein levels using RT-qPCR and western blot (**Figure 2F**, **2G**).

THOC2 knockdown reduces tumor growth and increases survival in mice with 5-FU resistant GBM

Upon establishing the correlation between 5-FU resistance and THOC2 expression, we

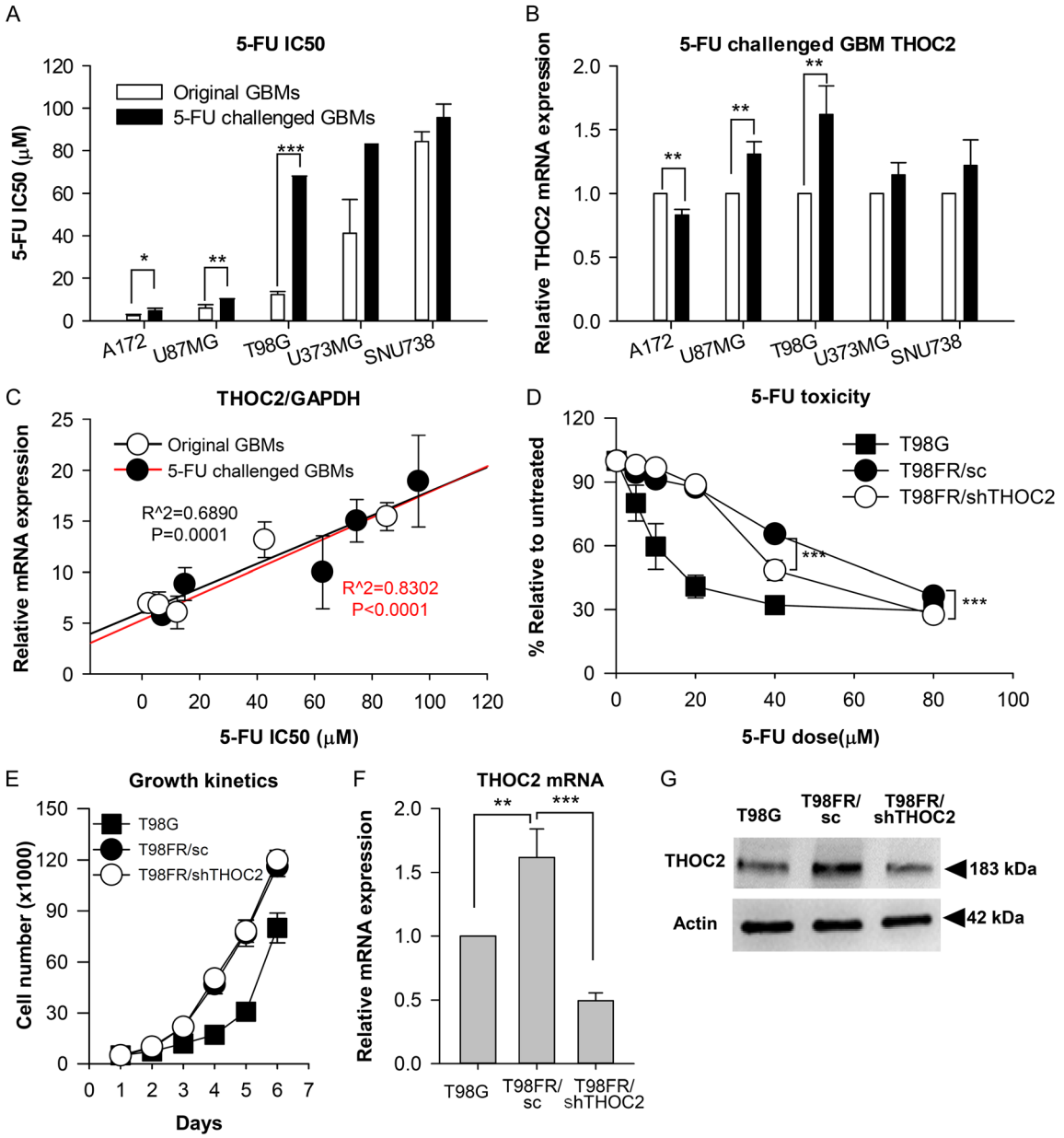

Figure 2. Characteristics of 5-FU resistant acquired T98FR cells. A, B. GBM cells were exposed to 5-FU for 12 months to develop resistance. Notably, T98FR cells showed a significant increase in 5-FU resistance and upregulated THOC2 expression. C. Linear regression analysis showing the correlation between 5-FU IC50 values and THOC2 mRNA expression levels in GBM cells both before and after 5-FU challenge. Open circles and black regression line represent original GBM cells, while filled circles and red regression line represent 5-FU challenged GBM cells. R^2 values and *P*-values are also shown on the graph in matching colors. D. T98G, T98FR/sc, and T98FR/shTHOC2 were cultured in the presence of the indicated concentrations of 5-FU for 72 hr. Surviving cells were quantified by MTT assays and presented as relative survival with respect to the value in the absence of 5-FU (student's t-test; **P < 0.01, ***P < 0.001). E. T98G, T98FG/sc, and T98FR/shTHOC2 growth rate comparison. Error bars indicate the SD. F, G. Relative mRNA expression level and protein level of THOC2 were quantified by RT-qPCR and western blot.

aimed to elucidate the functional role of THOC2 knockdown on 5-FU resistance using the T98FR cell line. To address this, we employed a T98FR subcutaneous xenograft model in 8-week-old NSG (NOD.Cg-Prkdcscid Il2rgtm1Wjl/SzJ) mice. T98FR/sc and T98FR/shTHOC2 cells were inoculated into the right flank of the mice, and following tumor formation, either saline or 80 mg/kg 5-FU was administered peritumorally once a week for three weeks. Our findings

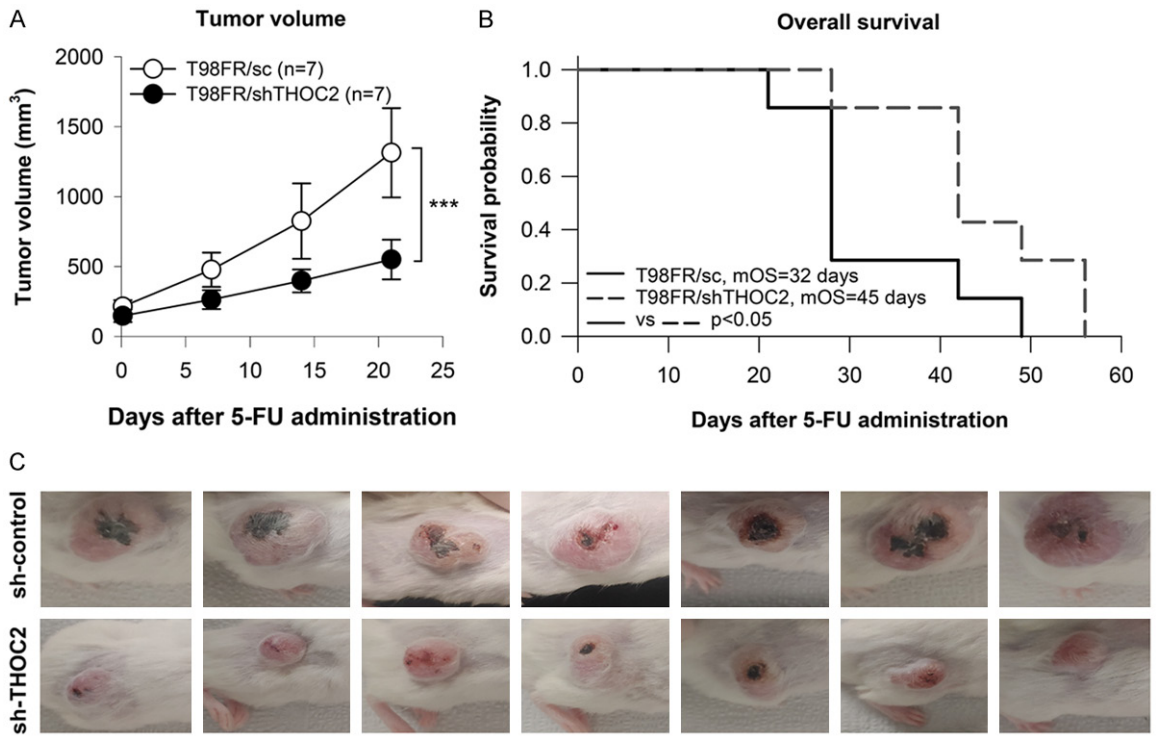

Figure 3. Effect of THOC2 knockdown in T98FR subcutaneous xenograft model. A. T98FR/sc and T98FR/shTHOC2 (1.5 × 10^6 cells, 20% matrigel) were inoculated into the right flank of NSG mice. After tumor formation, 80 mg/kg 5-FU was administered peritumorally, and tumor volume was measured once a week, for 3 weeks (student's t-test; ***P < 0.001). B. Overall survival of at least seven animals/group represented in Kaplan-Meier graph (Log-rank test; *P < 0.05). C. Tumor images of T98FR/sc and T98FR/shTHOC2 at 21 days after initial 5-FU treatment.

revealed that THOC2 knockdown markedly attenuated tumor growth in the 5-FU treated group, with the average tumor volume decreasing from 1,319 mm^3 to 597 mm^3 at 21 days post initial 5-FU administration ($P < 0.001$; **Figure 3A**, **3C**). Additionally, the Kaplan-Meier survival analysis demonstrated that THOC2 knockdown extended the average survival duration of NSG mice from 32 days to 45 days after the commencement of 5-FU treatment ($P < 0.05$; **Figure 3B**).

Identification of differentially expressed genes and splicing variants in T98FR and T98FR/shTHOC2 cells

To elucidate the molecular basis underlying the observed phenotypic changes in T98FR/shTHOC2 cells, we conducted RNA sequencing to identify differentially expressed genes and alternative splicing variants. Initially, we compared the expression levels of alternative splicing variants for each gene. A total of 2,433 transcripts displaying a correlation between 5-FU IC50 and normalized FPKM values ($P < 0.05$) were selected and subjected to functional annotation analysis. This analysis uncovered ten novel ontology terms associated with 5-FU sensitivities of T98G, T98FR/sc, and T98FR/shTHOC2 (**Figure 4A**, **4B**). We then extracted a list of transcripts involved in apoptotic processes, exhibiting the highest correlation between 5-FU IC50 and FPKM values ($P < 0.01$; **Figure 4C**).

Additionally, we compared gene expression changes between T98FR/sc and T98FR/shTHOC2 by hierarchical clustering (**Figure 4D**) and DEG analysis (**Figure 4E**). We identified ten biological process ontology terms with the highest statistical reliability and found cell adhesion to be the top among them ($P < 0.001$; **Figure 4E**). In addition to these findings, we identified genes with the most statistically significant decrease in T98FR/shTHOC2 compared to T98FR/sc among cell adhesion genes ($P < 0.001$; **Figure 4F**). These results provide a comprehensive view of the genes and splicing variants impacted by THOC2 expression, offering insights into the molecular mechanisms

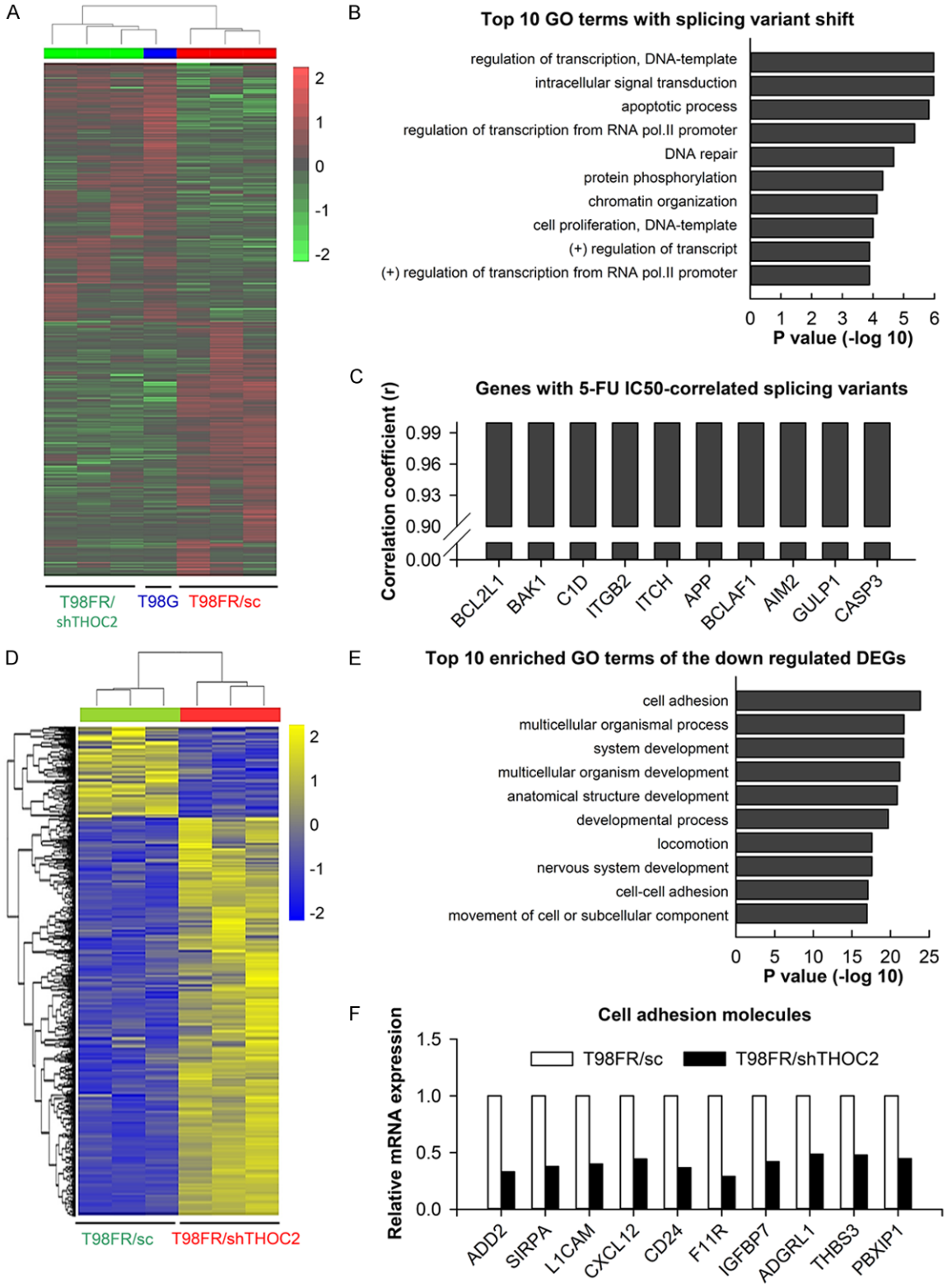

Figure 4. Analysis of differentially expressed genes and splicing variants in T98FR and T98FR/shTHOC2 cells. A. Hierarchical clustering heat map depicting splicing variants according to correlation with 5-FU IC50. B. Top 10 gene ontology terms exhibiting the highest correlation between expression levels and 5-FU IC50 values. C. Transcript variants in apoptotic process genes with the highest correlation between expression levels and 5-FU IC50 values. D. Hierarchical clustering heat map of DEGs between T98FR/sc and T98FR/shTHOC2. E. Top 10 enriched gene ontology terms (biological process) of the down regulated DEGs. F. Genes with the most significant decrease in T98FR/shTHOC2 compared to T98FR/sc among cell adhesion genes.

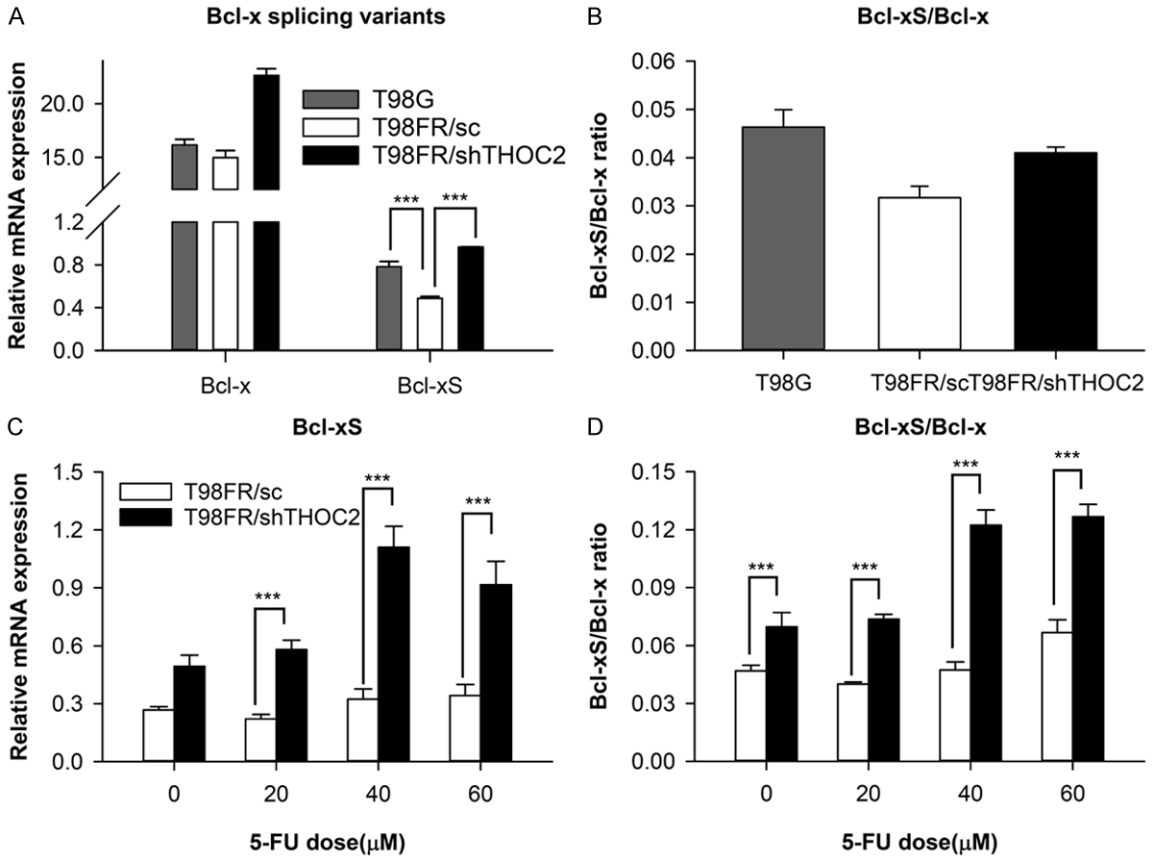

Figure 5. Knockdown of THOC2 in T98FR leads to a shift in alternative splicing variants of apoptosis-related gene, Bcl-x. Expression of the Bcl-x splicing variant was examined on day 2 following 5-FU treatment in three cell lines: T98G, T98FR/sc, and T98FR/shTHOC2. (A and B) show the RT-qPCR results of the Bcl-x splicing variant expressed in the three cell types under culture conditions, while (C and D) display the RT-qPCR results of the Bcl-x splicing variant expressed in T98FR/sc, and T98FR/shTHOC2 treated with 5-FU at the indicated concentrations (Student's t-test; ***P < 0.001).

underlying the phenotypic changes observed in T98FR/shTHOC2 cells.

THOC2 knockdown alters Bcl-x splicing and increases pro-apoptotic Bcl-xS expression in GBM cell lines

Among the alternative splicing variant changes observed in the RNA sequencing results, we selected Bcl-x, a gene closely related to apoptosis, as a candidate gene correlated with THOC2 expression. We assessed the relative mRNA expression levels of Bcl-x and its pro-apoptotic splicing variant, Bcl-xS, using RT-qPCR and determined the Bcl-xS/Bcl-x ratio (**Figure 5A**, **5B**). We exposed T98FR/sc and T98FR/shTHOC2 cells to 0, 20, 40, and 60 μM 5-FU for 48 hours and measured the relative mRNA expression levels of Bcl-x and Bcl-xS using RT-qPCR. T98FR/shTHOC2 displayed increased Bcl-xS expression compared to T98FR/sc ($P < 0.001$) under presence of 5-FU. Moreover, the Bcl-xS/Bcl-x ratio was higher in T98FR/shTHOC2 than in T98FR/sc across all tested conditions ($P < 0.001$; **Figure 5C**, **5D**).

THOC2 knockdown impairs cell adhesion and reduces L1CAM expression in GBM cell lines

Consistent with the RNA sequencing findings, T98FR/shTHOC2 cells exhibited impaired cell adhesion and delayed tumor formation, taking 80 days to form an initial tumor volume of 100 mm^3 compared to just 32 days for T98FR/sc cells ($P < 0.001$; **Figure 6A**). We examined L1CAM protein expression levels during early tumor formation (on day 42 for T98FR/sc) and when tumor volumes were similar (on day 90 for T98FR/shTHOC2, which corresponded to the tumor size of T98FR/sc on day 42) using

immunohistochemistry. The IHC images demonstrated decreased L1CAM expression in T98FR/shTHOC2 tumors at both these stages (**Figure 6B**). Additionally, we evaluated L1CAM expression levels in two cell lines, T98FR/sc and T98FR/shTHOC2, using RT-qPCR. Knockdown of THOC2 resulted in a decrease in L1CAM expression ($P < 0.001$; **Figure 6C**).

To validate the actual impact of THOC2 knockdown on cell adhesion, we performed cell attachment and wound healing assays. These experiments revealed a 30% reduction in cell attachment ability ($P < 0.01$; **Figure 6D**, **6E**) and a 20% decrease in migration ability ($P < 0.01$; **Figure 6F**, **6G**) in T98FR/shTHOC2 cells compared to control cells.

Discussion

In this study, we aimed to investigate the role of THOC2 in glioblastoma multiforme (GBM) cells' resistance to 5-fluorouracil (5-FU) and its potential as a therapeutic target. Our findings provide evidence for the involvement of THOC2 in 5-FU resistance and its impact on tumor growth, consistent with previous reports highlighting the heterogeneity in GBM and its impact on treatment response [26-28].

The observed correlation between cell doubling times and 5-FU IC50 values supports our hypothesis that THOC2 might be involved in 5-FU resistance. This finding aligns with previous studies implicating THO Complex Members in chemoresistance in other cancer types, such as hepatocellular carcinoma [29, 30]. Our results indicate that knocking down THOC2 in T98FR cells led to a decrease in 5-FU sensitivity, further reinforcing the role of THOC2 in 5-FU resistance.

In our experimental animal models, we demonstrated that THOC2 knockdown significantly suppressed tumor growth in the 5-FU treated group and extended the survival duration of the mice (**Figure 3A**, **3B**). These findings support the original hypothesis and suggest that targeting THOC2 could be a potential therapeutic strategy for overcoming 5-FU resistance in GBM, consistent with prior studies on the therapeutic potential of THOC2 inhibition [17, 18]. To further validate these results and to rule out potential off-target effects of the shRNA construct, we utilized a second shRNA targeting THOC2. This additional shRNA construct yielded consistent results, confirming the changes in 5-FU IC50, Bcl-x, and L1CAM expression that were observed with the original shRNA (Supplementary Figure 2). This consistency across different shRNA constructs provides robust support for our findings and reduces the likelihood of off-target effects skewing our interpretations. The results from the additional shRNA experiments have been included in the supplementary data to further substantiate our conclusions.

We identified differentially expressed genes and splicing variants in T98FR and T98FR/shTHOC2 cells. We found that THOC2 knockdown increased the expression of Bcl-xS, an apoptosis-related gene, in GBM cells. This result suggests a potential link between THOC2 and the regulation of apoptotic pathways, which could have implications for chemoresistance, although further research is needed to establish a direct connection with 5-FU resistance. Additionally, our study revealed that THOC2 expression is positively correlated with 5-FU resistance in GBM cell lines (**Figure 1F**). Notably, DPYD and TS, known as resistant factors to 5-FU [31-33], are not involved in 5-FU sensitivity of GBM. This new finding suggests that higher THOC2 levels contribute to reduced sensitivity to 5-FU treatment and that targeting THOC2 could be a viable therapeutic strategy to overcome 5-FU resistance in GBM patients.

Our study provides comprehensive evidence for the role of THOC2 in regulating 5-FU resistance and tumor formation in GBM through a combination of *in vitro* and *in vivo* experiments. We demonstrated that THOC2 suppression not only reduces tumor growth *in vivo* but also decreases the expression of cell-adhesion related genes, including L1CAM (**Figure 4E**), which subsequently impacts cell attachment and wound healing functions *in vitro* (**Figure 6E**, **6G**). The reduction in L1CAM expression, a molecule known to promote tumor cell invasion and motility [34], suggests that THOC2 may modulate GBM tumor invasiveness by regulating cell-adhesion related genes. Previous studies have reported that aberrant L1CAM expression is associated with poor prognosis in various cancer types [35], further supporting the potential significance of our findings. We also observed a decrease in L1CAM expression in

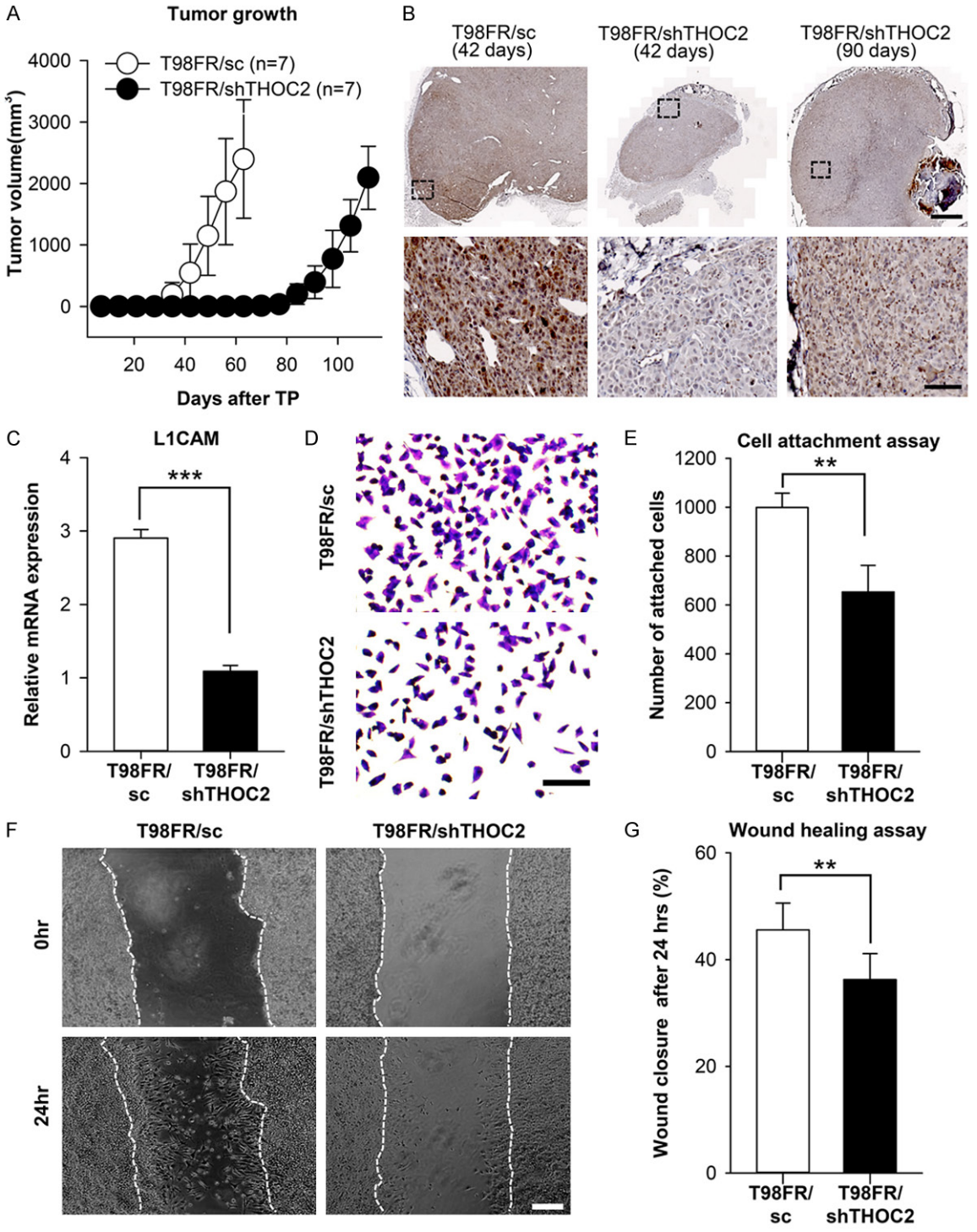

Figure 6. Reduced cell adhesion and retarded tumor formation in T98FR/shTHOC2. (A) *In vivo* tumor growth comparison following cell transplantation without any treatment. (B) L1CAM expression analysis via immunohistochemical staining at different time points post T98FR/sc or T98FR/shTHOC2 cell injection. Parenthetical numbers represent days after cell transplantation when animals were sacrificed. Upper panel: low-magnification image; lower panel: enlarged view of area denoted by dotted box. (C) L1CAM expression analysis via RT-qPCR in T98FR/sc and T98FR/shTHOC2 cells, with a statistically significant decrease in L1CAM expression in T98FR/shTHOC2 cells denoted by ***P < 0.001. (D) Attachment of T98FR/sc and T98FR/shTHOC2 cells to Matrigel-coated wells for 6 hours, followed by washing, fixing, and crystal violet staining. (E) Quantitative comparison of attached cell counts between T98FR/sc and T98FR/shTHOC2. (F) Scratch wound assay performed 24 hours post serum starvation of T98FR/sc and

T98FR/shTHOC2 cells, with incubation continuing for an additional 24 hours. (G) Quantitative comparison of wound closure percentages between T98FR/sc and T98FR/shTHOC2. Scale bars: B (upper panel) = 1,000 μm; B (lower panel), D = 100 μm; F = 200 μm. Statistical comparisons in (E and G) were analyzed using Student's t-test with **P < 0.01 indicating significant differences.

T98FR/shTHOC2 cells with reduced tumor formation, which is noteworthy since various cell adhesion molecules, including L1CAM, are required for orthotopic tumor engraftment [36]. Moreover, L1CAM might not be the only cell adhesion molecule influencing cell engraftment. Although not a cancer case, Integrin subunit beta 2 (ITGB2), which showed a 3-fold decrease in T98FR/shTHOC2, has been reported to improve survival and engraftment of adipose stem cells into infarcted myocardium [37]. We hypothesize that THOC2 knockdown leads to a decrease in cell adhesion molecules, thereby inhibiting tumor cell engraftment in the orthotopic model. In addition to the effects of L1CAM and other cell adhesion molecules on tumor engraftment, we believe that these molecules also play a role in cancer cell survival. For instance, CD24, one of the top 10 significantly decreased cell adhesion molecules in T98FR/shTHOC2, has been reported to regulate cancer cell proliferation and immune evasion [38, 39]. Meanwhile, CXCL12, another top 10 adhesion molecule, is known to promote chemoresistance in cancer [40].

The THO/TREX complex is a crucial protein aggregate involved in post-transcriptional RNA processing and translocation [41]. It plays a significant role in the nucleo-cytoplasmic transition that occurs during mRNA translocation out of the nuclear space [42]. Although the THO complex has been implicated in alternative RNA splicing in plants [43, 44], its role in mammalian cells or THOC2 has not been reported. In this study, we investigated the splicing variants of apoptosis-related genes in cells with THOC2 knockdown through RNA sequencing and observed a change in Bcl-x. Bcl proteins can exhibit either pro- or anti-apoptotic properties depending on the Bcl-2 homology (BH) domains present. Bcl-x is a member of the Bcl-2 family of proteins containing multiple BH3 domains and is regulated by pro-apoptotic Bcl-xS and anti-apoptotic Bcl-xL through alternative splicing [45]. Our results indicated that THOC2 suppression led to an increase in the expression of pro-apoptotic protein Bcl-xS in GBM cell lines following 5-FU treatment. This suggests that elevated THOC2 may suppress Bcl-x alternative splicing to Bcl-xS. We confirmed Bcl-x alternative splicing using qPCR with primers specifically designed to detect it. The increase in Bcl-xS expression upon THOC2 knockdown could be one of the mechanisms by which THOC2 influences GBM tumor growth and response to 5-FU treatment. This observation is consistent with previous research showing that the balance between pro- and anti-apoptotic factors plays a critical role in determining cell fate and therapy response [46]. However, additional studies are needed to determine whether THOC2 directly regulates alternative splicing of Bcl-x. Besides Bcl-x or other apoptosis-related genes, it is also noteworthy that the expression of DNA repair transcripts correlates with THOC2 expression, as glioma cells are known to develop resistance to DNA damage through the activation of DNA damage responses [47].

Our results reveal that THOC2 knockdown reduced cell adhesion and L1CAM expression in GBM cells suggest a potential role for THOC2 in the aggressiveness of GBM tumors. This finding is in line with other studies that have established a connection between L1CAM expression and tumor progression and metastasis [48, 49]. The functional consequences of altered Bcl-xS and L1CAM expression upon THOC2 knockdown should be explored through *in vitro* and *in vivo* functional assays to validate their roles in GBM tumor growth and 5-FU resistance. Additionally, the potential interactions between THOC2 and other signaling pathways or molecular regulators should be examined to gain a comprehensive understanding of its role in GBM tumor biology and chemoresistance.

In conclusion, our study provides evidence for the role of THOC2 in 5-FU resistance and tumor formation in GBM. We demonstrated that THOC2 suppression led to increased 5-FU sensitivity, reduced tumor growth, and altered expression of apoptosis-related genes and cell adhesion molecules in GBM cells. Our findings suggest that targeting THOC2 could be a potential therapeutic strategy to overcome 5-FU resistance in GBM patients. Future studies should investigate the precise mechanisms by

which THOC2 modulates alternative splicing of Bcl-x and the expression of cell adhesion molecules like L1CAM. Moreover, the potential crosstalk between THOC2 and other signaling pathways or molecular regulators should be explored to develop a comprehensive understanding of its role in GBM tumor biology and chemoresistance. Our study lays the foundation for further research on THOC2 as a potential target for overcoming chemoresistance and improving treatment outcomes for GBM patients.

It is worth noting that, although our study has provided valuable insights into the role of THOC2 in GBM, there are several limitations that should be addressed in future research. First, the use of more diverse GBM cell lines and patient-derived samples would provide a more comprehensive understanding of THOC2's role in 5-FU resistance across a broader range of GBM cases. Second, our study focused mainly on the role of THOC2 in 5-FU resistance, but it is essential to investigate whether THOC2 also plays a role in resistance to other chemotherapeutic agents commonly used in GBM treatment. Finally, it would be beneficial to explore the therapeutic potential of THOC2 inhibition in combination with other targeted therapies, to determine whether a synergistic effect might be achieved in overcoming GBM chemoresistance.

Acknowledgements

This study was supported by grants of Basic Science Research Program through NRF funded by the Ministry of Education, Science and Technology (NRF-2020R1I1A1A010731-37); and Korea Drug Development Fund funded by Ministry of Science and ICT, Ministry of Trade, Industry, and Energy, and Ministry of Health and Welfare (RS-2022-00165974).

Disclosure of conflict of interest

J.J.H., D.Y.C., N.B., and H.S.K. are employees of and stock and/or option holders in Cell&Brain Co., Ltd. The other authors have no potential conflicts of interest to disclose.

Address correspondence to: Drs. Haeyoung Suh-Kim and Sung-Soo Kim, Department of Anatomy, Ajou University School of Medicine, 164, World Cup-ro, Yeongtong-gu, Suwon 16499, South Korea. Tel: 82-31-219-5033; Fax: 82-31-219-5039; E-mail: hysuh@ajou.ac.kr (HSK); Tel: 82-31-219-5034; Fax: 82-31-219-5039; E-mail: kimdmg@ajou.ac.kr (SSK)

References

[1] Rock K, McArdle O, Forde P, Dunne M, Fitzpatrick D, O'Neill B and Faul C. A clinical review of treatment outcomes in glioblastoma multiforme--the validation in a non-trial population of the results of a randomised phase III clinical trial: has a more radical approach improved survival? Br J Radiol 2012; 85: e729-733.

[2] Ostrom QT, Gittleman H, Liao P, Vecchione-Koval T, Wolinsky Y, Kruchko C and Barnholtz-Sloan JS. CBTRUS statistical report: primary brain and other central nervous system tumors diagnosed in the United States in 2010-2014. Neuro Oncol 2017; 19: v1-v88.

[3] Ohka F, Natsume A and Wakabayashi T. Current trends in targeted therapies for glioblastoma multiforme. Neurol Res Int 2012; 2012: 878425.

[4] Thakkar JP, Dolecek TA, Horbinski C, Ostrom QT, Lightner DD, Barnholtz-Sloan JS and Villano JL. Epidemiologic and molecular prognostic review of glioblastoma. Cancer Epidemiol Biomarkers Prev 2014; 23: 1985-1996.

[5] Stupp R, Taillibert S, Kanner A, Read W, Steinberg D, Lhermitte B, Toms S, Idbaih A, Ahluwalia MS, Fink K, Di Meco F, Lieberman F, Zhu JJ, Stragliotto G, Tran D, Brem S, Hottinger A, Kirson ED, Lavy-Shahaf G, Weinberg U, Kim CY, Paek SH, Nicholas G, Bruna J, Hirte H, Weller M, Palti Y, Hegi ME and Ram Z. Effect of tumor-treating fields plus maintenance temozolomide vs maintenance temozolomide alone on survival in patients with glioblastoma: a randomized clinical trial. JAMA 2017; 318: 2306-2316.

[6] Alexander BM and Cloughesy TF. Adult glioblastoma. J Clin Oncol 2017; 35: 2402-2409.

[7] Weller M, Cloughesy T, Perry JR and Wick W. Standards of care for treatment of recurrent glioblastoma--are we there yet? Neuro Oncol 2013; 15: 4-27.

[8] Sarkaria JN, Hu LS, Parney IF, Pafundi DH, Brinkmann DH, Laack NN, Giannini C, Burns TC, Kizilbash SH, Laramy JK, Swanson KR, Kaufmann TJ, Brown PD, Agar NYR, Galanis E, Buckner JC and Elmquist WF. Is the blood-brain barrier really disrupted in all glioblastomas? A critical assessment of existing clinical data. Neuro Oncol 2018; 20: 184-191.

[9] Shinde G, Shiyani S, Shelke S, Chouthe R, Kulkarni D and Marvaniya K. Enhanced brain targeting efficiency using 5-FU (fluorouracil) lipid-drug conjugated nanoparticles in brain cancer therapy. Prog Biomater 2020; 9: 259-275.

[10] Pandey A, Kulkarni S, Vincent AP, Nannuri SH, George SD and Mutalik S. Hyaluronic acid-drug conjugate modified core-shell MOFs as pH responsive nanoplatform for multimodal therapy of glioblastoma. Int J Pharm 2020; 588: 119735.
[11] Lakkadwala S and Singh J. Dual functionalized 5-fluorouracil liposomes as highly efficient nanomedicine for glioblastoma treatment as assessed in an in vitro brain tumor model. J Pharm Sci 2018; 107: 2902-2913.
[12] Philbrick BD and Adamson DC. Early clinical trials of Toca 511 and Toca FC show a promising novel treatment for recurrent malignant glioma. Expert Opin Investig Drugs 2019; 28: 207-216.
[13] Chang DY, Jung JH, Kim AA, Marasini S, Lee YJ, Paek SH, Kim SS and Suh-Kim H. Combined effects of mesenchymal stem cells carrying cytosine deaminase gene with 5-fluorocytosine and temozolomide in orthotopic glioma model. Am J Cancer Res 2020; 10: 1429-1441.
[14] Chang DY, Yoo SW, Hong Y, Kim S, Kim SJ, Yoon SH, Cho KG, Paek SH, Lee YD, Kim SS and Suh-Kim H. The growth of brain tumors can be suppressed by multiple transplantation of mesenchymal stem cells expressing cytosine deaminase. Int J Cancer 2010; 127: 1975-1983.
[15] Katahira J. mRNA export and the TREX complex. Biochim Biophys Acta 2012; 1819: 507-513.
[16] Chi B, Wang Q, Wu G, Tan M, Wang L, Shi M, Chang X and Cheng H. Aly and THO are required for assembly of the human TREX complex and association of TREX components with the spliced mRNA. Nucleic Acids Res 2013; 41: 1294-1306.
[17] Zhou X, Liu X, Zhang G, Zhang Q, Chen H, Wang Y, Fang F and Sun J. Knockdown THOC2 suppresses the proliferation and invasion of melanoma. Bioengineered 2019; 10: 635-645.
[18] Bai X, Ni J, Beretov J, Wang S, Dong X, Graham P and Li Y. THOC2 and THOC5 regulate stemness and radioresistance in triple-negative breast cancer. Adv Sci (Weinh) 2021; 8: e2102658.
[19] Longley DB, Harkin DP and Johnston PG. 5-fluorouracil: mechanisms of action and clinical strategies. Nat Rev Cancer 2003; 3: 330-338.
[20] Takahashi M, Valdes G, Hiraoka K, Inagaki A, Kamijima S, Micewicz E, Gruber HE, Robbins JM, Jolly DJ, McBride WH, Iwamoto KS and Kasahara N. Radiosensitization of gliomas by intracellular generation of 5-fluorouracil potentiates prodrug activator gene therapy with a retroviral replicating vector. Cancer Gene Ther 2014; 21: 405-410.
[21] Robinson MD, McCarthy DJ and Smyth GK. edgeR: a bioconductor package for differential expression analysis of digital gene expression data. Bioinformatics 2010; 26: 139-140.
[22] Raudvere U, Kolberg L, Kuzmin I, Arak T, Adler P, Peterson H and Vilo J. g:Profiler: a web server for functional enrichment analysis and conversions of gene lists (2019 update). Nucleic Acids Res 2019; 47: W191-W198.
[23] Huang da W, Sherman BT and Lempicki RA. Systematic and integrative analysis of large gene lists using DAVID bioinformatics resources. Nat Protoc 2009; 4: 44-57.
[24] Sherman BT, Hao M, Qiu J, Jiao X, Baseler MW, Lane HC, Imamichi T and Chang W. DAVID: a web server for functional enrichment analysis and functional annotation of gene lists (2021 update). Nucleic Acids Res 2022; 50: W216-221.
[25] Ge SX, Son EW and Yao R. iDEP: an integrated web application for differential expression and pathway analysis of RNA-Seq data. BMC Bioinformatics 2018; 19: 534.
[26] Verhaak RG, Hoadley KA, Purdom E, Wang V, Qi Y, Wilkerson MD, Miller CR, Ding L, Golub T, Mesirov JP, Alexe G, Lawrence M, O'Kelly M, Tamayo P, Weir BA, Gabriel S, Winckler W, Gupta S, Jakkula L, Feiler HS, Hodgson JG, James CD, Sarkaria JN, Brennan C, Kahn A, Spellman PT, Wilson RK, Speed TP, Gray JW, Meyerson M, Getz G, Perou CM and Hayes DN; Cancer Genome Atlas Research Network. Integrated genomic analysis identifies clinically relevant subtypes of glioblastoma characterized by abnormalities in PDGFRA, IDH1, EGFR, and NF1. Cancer Cell 2010; 17: 98-110.
[27] Sottoriva A, Spiteri I, Piccirillo SG, Touloumis A, Collins VP, Marioni JC, Curtis C, Watts C and Tavaré S. Intratumor heterogeneity in human glioblastoma reflects cancer evolutionary dynamics. Proc Natl Acad Sci U S A 2013; 110: 4009-4014.
[28] Aldape K, Zadeh G, Mansouri S, Reifenberger G and von Deimling A. Glioblastoma: pathology, molecular mechanisms and markers. Acta Neuropathol 2015; 129: 829-848.
[29] Cai S, Bai Y, Wang H, Zhao Z, Ding X, Zhang H, Zhang X, Liu Y, Jia Y, Li Y, Chen S, Zhou H, Liu H, Yang C and Sun T. Knockdown of THOC1 reduces the proliferation of hepatocellular carcinoma and increases the sensitivity to cisplatin. J Exp Clin Cancer Res 2020; 39: 135.
[30] Li X, Liu Z, Wei X, Lin J, Yang Q and Xie Y. Comprehensive analysis of the expression and clinical significance of THO complex members in hepatocellular carcinoma. Int J Gen Med 2022; 15: 2695-2713.
[31] Cho HJ, Park YS, Kang WK, Kim JW and Lee SY. Thymidylate synthase (TYMS) and dihydropy-

rimidine dehydrogenase (DPYD) polymorphisms in the Korean population for prediction of 5-fluorouracil-associated toxicity. Ther Drug Monit 2007; 29: 190-196.
[32] Amstutz U, Froehlich TK and Largiader CR. Dihydropyrimidine dehydrogenase gene as a major predictor of severe 5-fluorouracil toxicity. Pharmacogenomics 2011; 12: 1321-1336.
[33] Detailleur S, Segelov E, Re MD and Prenen H. Dihydropyrimidine dehydrogenase deficiency in patients with severe toxicity after 5-fluorouracil: a retrospective single-center study. Ann Gastroenterol 2021; 34: 68-72.
[34] Gavert N and Ben-Ze'ev A. Epithelial-mesenchymal transition and the invasive potential of tumors. Trends Mol Med 2008; 14: 199-209.
[35] Mechtersheimer S, Gutwein P, Agmon-Levin N, Stoeck A, Oleszewski M, Riedle S, Postina R, Fahrenholz F, Fogel M, Lemmon V and Altevogt P. Ectodomain shedding of L1 adhesion molecule promotes cell migration by autocrine binding to integrins. J Cell Biol 2001; 155: 661-673.
[36] Ganesh K, Basnet H, Kaygusuz Y, Laughney AM, He L, Sharma R, O'Rourke KP, Reuter VP, Huang YH, Turkekul M, Er EE, Masilionis I, Manova-Todorova K, Weiser MR, Saltz LB, Garcia-Aguilar J, Koche R, Lowe SW, Pe'er D, Shia J and Massagué J. L1CAM defines the regenerative origin of metastasis-initiating cells in colorectal cancer. Nat Cancer 2020; 1: 28-45.
[37] Yuan Z, Yan K and Wang J. Overexpression of integrin beta(2) improves migration and engraftment of adipose-derived stem cells and augments angiogenesis in myocardial infarction. Ann Transl Med 2022; 10: 863.
[38] Barkal AA, Brewer RE, Markovic M, Kowarsky M, Barkal SA, Zaro BW, Krishnan V, Hatakeyama J, Dorigo O, Barkal LJ and Weissman IL. CD24 signalling through macrophage Siglec-10 is a target for cancer immunotherapy. Nature 2019; 572: 392-396.
[39] Altevogt P, Sammar M, Huser L and Kristiansen G. Novel insights into the function of CD24: a driving force in cancer. Int J Cancer 2021; 148: 546-559.
[40] Shi Y, Riese DJ 2nd and Shen J. The role of the CXCL12/CXCR4/CXCR7 chemokine axis in cancer. Front Pharmacol 2020; 11: 574667.
[41] Masuda S, Das R, Cheng H, Hurt E, Dorman N and Reed R. Recruitment of the human TREX complex to mRNA during splicing. Genes Dev 2005; 19: 1512-1517.
[42] Köhler A and Hurt E. Exporting RNA from the nucleus to the cytoplasm. Nat Rev Mol Cell Biol 2007; 8: 761-773.
[43] Sun N, Kong X, Liu Y, Gong T, Gu X and Liu L. The THO/TREX complex active in alternative splicing mediates plant responses to salicylic acid and jasmonic acid. Int J Mol Sci 2021; 22: 12197.
[44] Meyer K, Koester T and Staiger D. Pre-mRNA splicing in plants: in vivo functions of RNA-binding proteins implicated in the splicing process. Biomolecules 2015; 5: 1717-1740.
[45] Boise LH, González-García M, Postema CE, Ding L, Lindsten T, Turka LA, Mao X, Nuñez G and Thompson CB. bcl-x, a bcl-2-related gene that functions as a dominant regulator of apoptotic cell death. Cell 1993; 74: 597-608.
[46] Hanahan D and Weinberg RA. Hallmarks of cancer: the next generation. Cell 2011; 144: 646-674.
[47] Bao S, Wu Q, McLendon RE, Hao Y, Shi Q, Hjelmeland AB, Dewhirst MW, Bigner DD and Rich JN. Glioma stem cells promote radioresistance by preferential activation of the DNA damage response. Nature 2006; 444: 756-760.
[48] Gavert N, Sheffer M, Raveh S, Spaderna S, Shtutman M, Brabletz T, Barany F, Paty P, Notterman D, Domany E and Ben-Ze'ev A. Expression of L1-CAM and ADAM10 in human colon cancer cells induces metastasis. Cancer Res 2007; 67: 7703-7712.
[49] Kiefel H, Bondong S, Hazin J, Ridinger J, Schirmer U, Riedle S and Altevogt P. L1CAM: a major driver for tumor cell invasion and motility. Cell Adh Migr 2012; 6: 374-384.
[50] Li Z, Li Q, Han L, Tian N, Liang Q, Li Y, Zhao X, Du C and Tian Y. Pro-apoptotic effects of splice-switching oligonucleotides targeting Bcl-x pre-mRNA in human glioma cell lines. Oncol Rep 2016; 35: 1013-1019.
[51] Singh R, Gupta SC, Peng WX, Zhou N, Pochampally R, Atfi A, Watabe K, Lu Z and Mo YY. Regulation of alternative splicing of Bcl-x by BC200 contributes to breast cancer pathogenesis. Cell Death Dis 2016; 7: e2262.

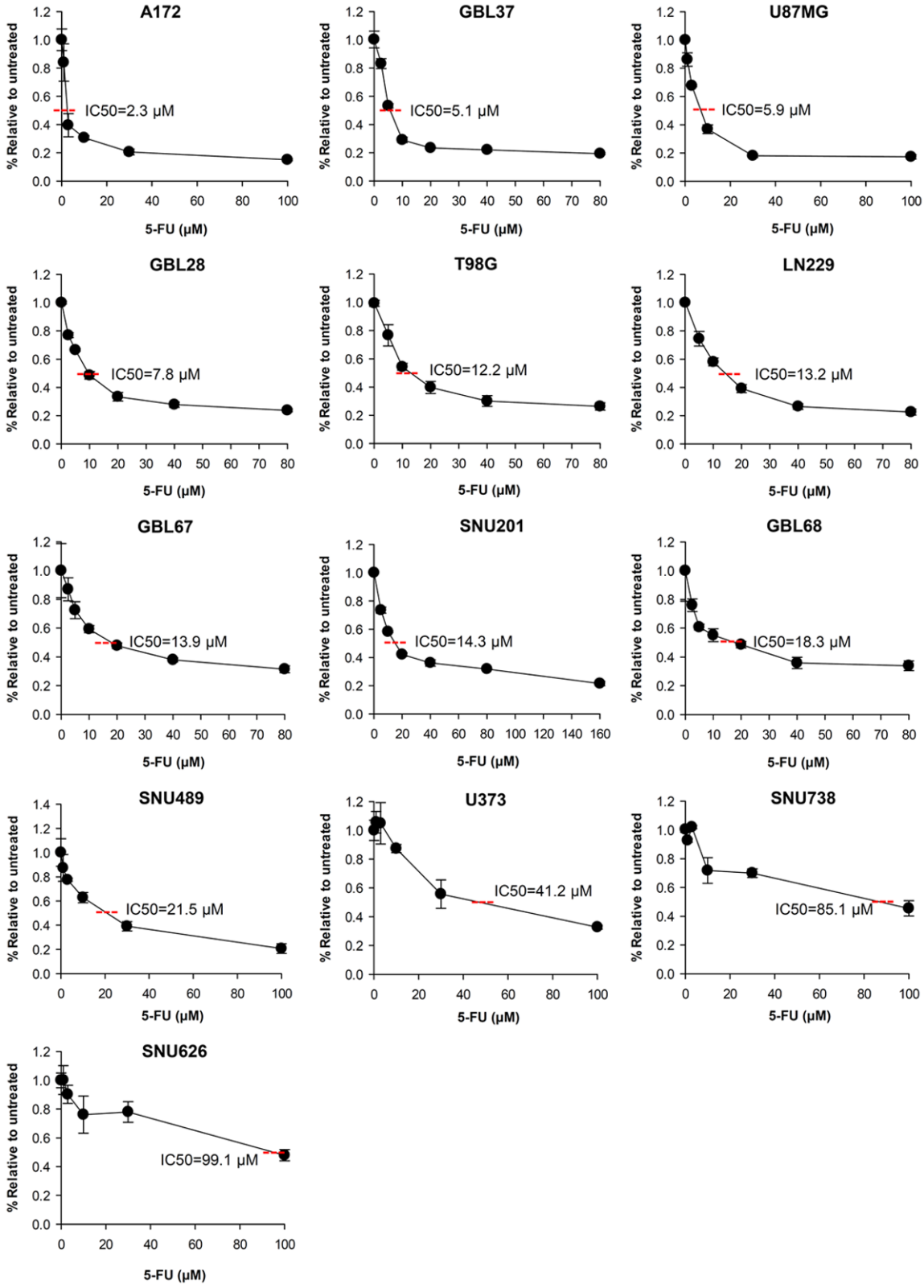

Supplementary Figure 1. Dose-response curves for GBM cell lines. The sensitivity of ten glioblastoma (GBM) cell lines to 5-fluorouracil (5-FU) was determined by generating dose-response curves. Each panel represents the dose-response curve of a specific GBM cell line, labeled accordingly. Each curve is derived from the mean ± SEM of three independent experiments. The calculated half-maximal inhibitory concentration (IC50) values for each cell line are indicated directly on the respective graphs.

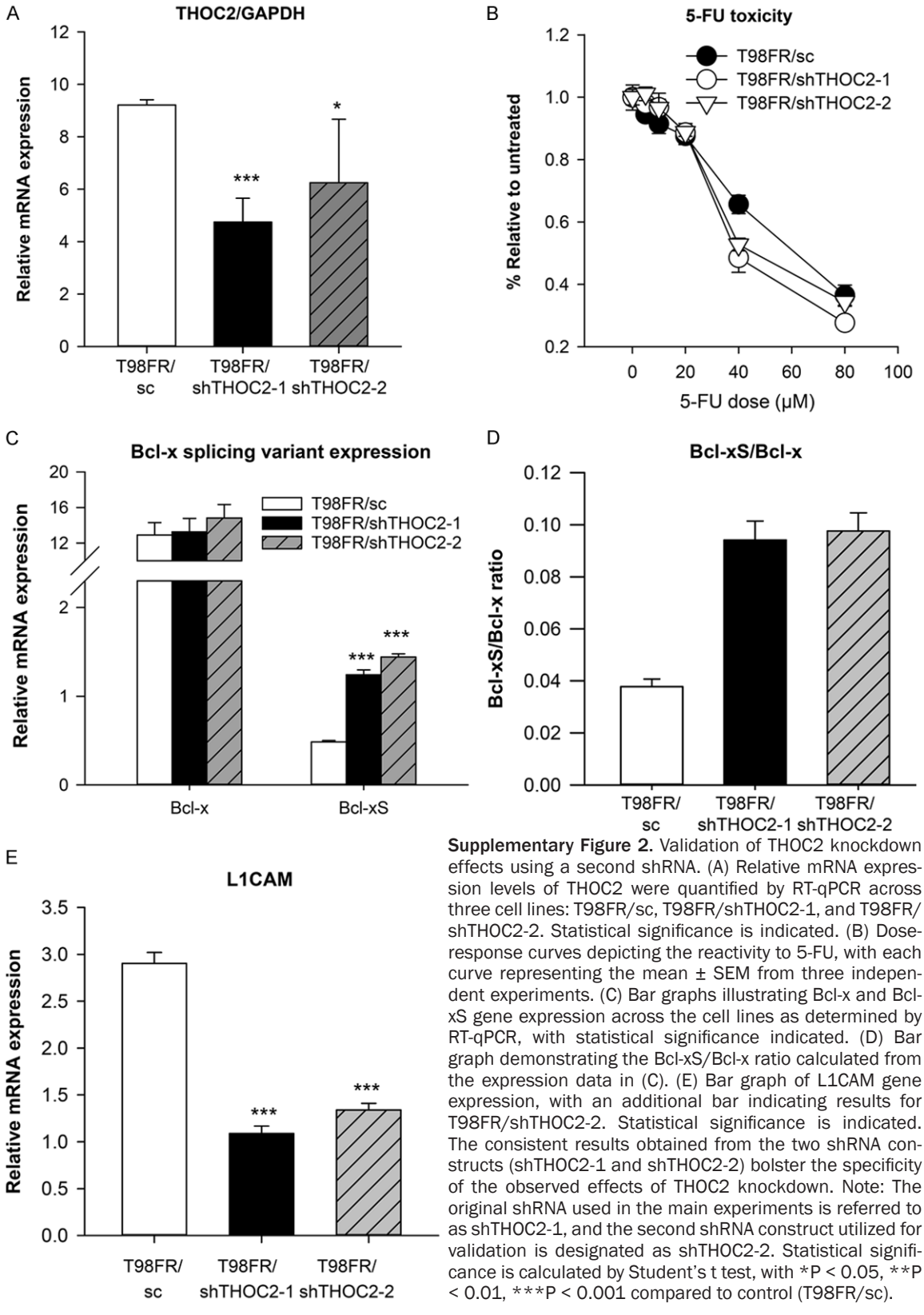

Supplementary Figure 2. Validation of THOC2 knockdown effects using a second shRNA. (A) Relative mRNA expression levels of THOC2 were quantified by RT-qPCR across three cell lines: T98FR/sc, T98FR/shTHOC2-1, and T98FR/shTHOC2-2. Statistical significance is indicated. (B) Dose-response curves depicting the reactivity to 5-FU, with each curve representing the mean ± SEM from three independent experiments. (C) Bar graphs illustrating Bcl-x and Bcl-xS gene expression across the cell lines as determined by RT-qPCR, with statistical significance indicated. (D) Bar graph demonstrating the Bcl-xS/Bcl-x ratio calculated from the expression data in (C). (E) Bar graph of L1CAM gene expression, with an additional bar indicating results for T98FR/shTHOC2-2. Statistical significance is indicated. The consistent results obtained from the two shRNA constructs (shTHOC2-1 and shTHOC2-2) bolster the specificity of the observed effects of THOC2 knockdown. Note: The original shRNA used in the main experiments is referred to as shTHOC2-1, and the second shRNA construct utilized for validation is designated as shTHOC2-2. Statistical significance is calculated by Student's t test, with *P < 0.05, **P < 0.01, ***P < 0.001 compared to control (T98FR/sc).